Rod-like Liquid Crystals of Organic Transition-metal Complexes

Part 4.†—Optically Positive Uniaxial Nematic Phase in the Bis[1-(4′-alkoxybiphenyl-4-yl)-3-alkylpropane-1,3-dionato]copper(II) Complexes

Kazuchika Ohta,* Hajime Akimoto, Tetsuya Fujimoto and Iwao Yamamoto
Department of Functional Polymer Science, Faculty of Textile Science & Technology, Shinshu University, Ueda 386, Japan

We report that the long-alkoxy-chain substituted bis(β-diketonato)copper(II) complexes, bis[1-(4′-dodecyloxybiphenyl-4-yl)-3-alkylpropane-1,3-dionato]copper(II) [alkyl substituent (R′): ethyl, *n*-propyl and *n*-butyl], show a nematic (N) phase. The methyl complex has a discotic rectangular ordered columnar (D_{ro}) phase, as reported previously. Therefore, the change from the D_{ro} phase to the N phase occurs with changing from R′ = methyl to R′ = ethyl groups. In order to obtain derivatives having a wider temperature range for the nematic phase, a homologous series of the bis[1-(4′-alkoxybiphenyl-4-yl)pentane-1,3-dionato]copper(II) complexes (alkoxy = $C_nH_{2n+1}O$; n = 6, 8, 10, 11, 14) have been synthesized for R′ = ethyl. The derivative for n = 11 gave the widest range (ΔT = 16.1 °C). Furthermore, the nematic phase of these complexes was established as an optically positive uniaxial nematic phase. The mesomorphism of the corresponding ligands was also investigated.

To date, several liquid-crystalline compounds containing a bis(β-diketonato)copper(II) complex core have been reported (Fig. 1). These complexes show a discotic lamellar (D_L) phase (1),[2–8] a discotic hexagonal (D_h) phase (2),[9,10] a discotic rectangular (D_r) phase (5),[11] and a nematic (N) phase (3–5),[12–17] It is very interesting that the bis(β-diketonato)copper(II) complexes, 5, which were recently reported by Ohta *et al.*, show a D_{ro} mesophase when the substituent R′ is a methyl group[11] and a monotropic N phase when the substituent R′ is an *n*-butyl group.[16]

In this paper we focus on phases of the complexes **11** (Scheme 1), with the substituent R′ ethyl or *n*-propyl. The new complexes with R′ ethyl or *n*-propyl have been synthesized and the effect of the alkyl chain (R′) on the mesomorphism has been investigated. It was found that these complexes show an enantiotropic N phase, and that the change from the D_{ro} phase to the N phase critically occurs with changing from the R′ = methyl group to R′ = ethyl group.

We synthesized a homologous series of the complexes **12** (n = 6, 8, 10, 11, 14; Scheme 1) to obtain derivatives with a wider temperature range for the nematic phase than that for complex **11** (m = 2). All the complexes **12** showed an enantiotropic nematic phase. The temperature range of the nematic phase of the n = 11 derivative (ΔT = 16.1 °C) is the widest for the derivatives. The conoscopic figures indicated that the present nematic phase is optically positive uniaxial.

We report here the interesting change from the D_{ro} phase to the nematic phase in the complexes **11**, and the optically positive uniaxial nematic phase in the complexes **12**.

Experimental

Synthesis

The synthetic route for the bis[1-(4′-alkoxybiphenyl-4-yl)-3-alkylpropane-1,3-dionato]copper(II) complexes (**11** and **12**) is shown in Scheme 1. 4-Alkoxy-4′-acetylbiphenyls (**8**) were obtained by the literature method.[18] The ligands **9** and **10** were synthesized by our previously reported method.[19] In Table 1 are listed the elemental analysis data and their yields. In Table 2 are listed elemental analysis data and yields of the complexes **11** and **12**. The detailed procedures of the representative ligand **10** (n = 8) and the complex, **12** (n = 12) are described in the following.

1-(4′-*Octyloxybiphenyl*-4-yl)*pentane*-1,3-*dione* (**10**, n = 8)
Sodium hydride (60%; 1.23 g, 30.8 mmol) was placed in a 100 cm^3 three-necked flask in a nitrogen atmosphere, and washed with dry hexane to remove the mineral oil. To this, were introduced 4-octyloxy-4′-acetylbiphenyl (5.00 g, 15.4 mmol) and then freshly distilled tetrahydrofuran (THF) (*ca.* 40 cm^3). After refluxing for *ca.* 2 h, the solution was cooled to room temperature (r.t.). Ethyl propionate (7.87 g, 77.1 mol)–THF(*ca.* 10 ml) was added dropwise to the solution, and refluxed again overnight (*ca.* 15 h). After it had been cooled to r.t., the reaction was stopped by adding 1 mol dm^{-3} hydrochloric acid (*ca.* 30 ml). The solvent was evaporated to give a yellow solid. The purification was carried out by column chromatography (silica gel, chloroform, R_f = 0.75) and recrystallization from ethyl acetate to give 3.42 g of light-yellow powder. Yield 58%. ^{1}H NMR(CDCl$_3$, TMS) δ_H 0.80–1.90 [m, 18 H, $CH_3(CH_2)_6$ CH$_2$O- and -COCH$_2$CH_3], 2.44 (q, 2 H, -COCH_2CH$_3$), 3.99 (t, 2 H, -CH_2O-), 6.15 (s, 1 H, enol CH), 6.85–7.98 (m, 8 H, biphenyl), 16.1 (s, 1 H, enol OH), keto: enol = 0:100.

Bis[1-4′-*dodecyloxybihenyl*-4-yl)*pentane*-1,3-*dionato*]*copper*(II) (**12**, n = 12)
β-Diketone, C_{12}O–Lig–Et (**10**, n = 12; 0.16 g, 0.37 mmol) and ethanol (*ca.* 15 ml) were placed in a 30 ml flask, and heated to dissolve. To this solution were added an aqueous solution of ammonium hydroxide (28%, *ca.* 1 ml) and an ethanolic solution of copper(II) chloride dihydrate (0.030 g, 0.19 mmol). The solution was refluxed for *ca.* 1 h. The reaction mixtures were filtered off, washed with hot water and hot ethanol, and dried *in vacuo*. The residue was purified by column chromatography (silica gel, chloroform, R_f = 0.78) and recrystallization from carbon tetrachloride to afford 0.11 g of grey-green powder: yield 64%.

Measurements

The phase-transition behaviour of the complexes **11** and **12** and their corresponding ligands were observed with a polarizing microscope (Olympus BH-2) equipped with a heating

† Part 3: ref. 1.

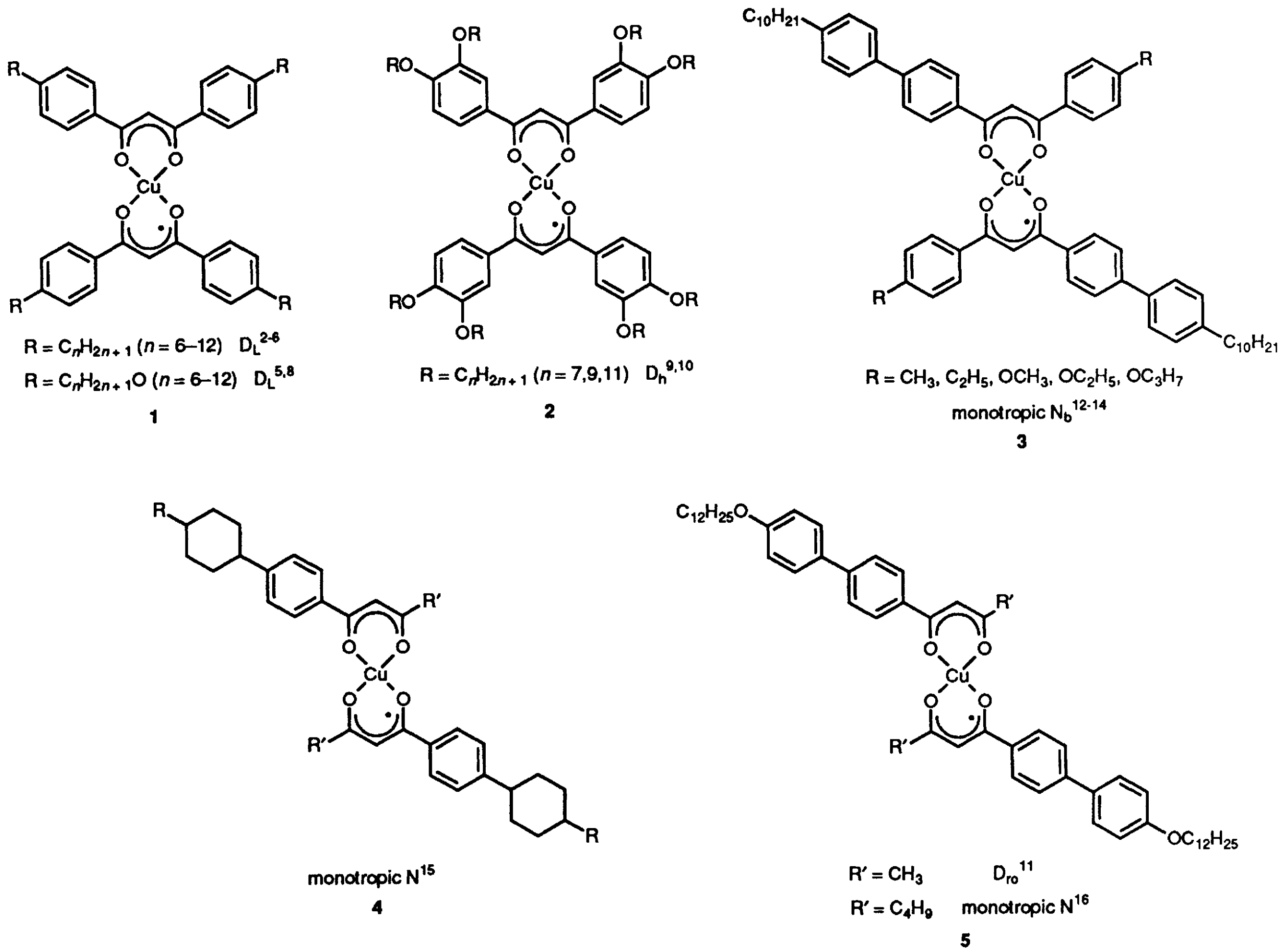

Fig. 1 Mesogenic bis(β-diketonato)copper(II) complex derivatives

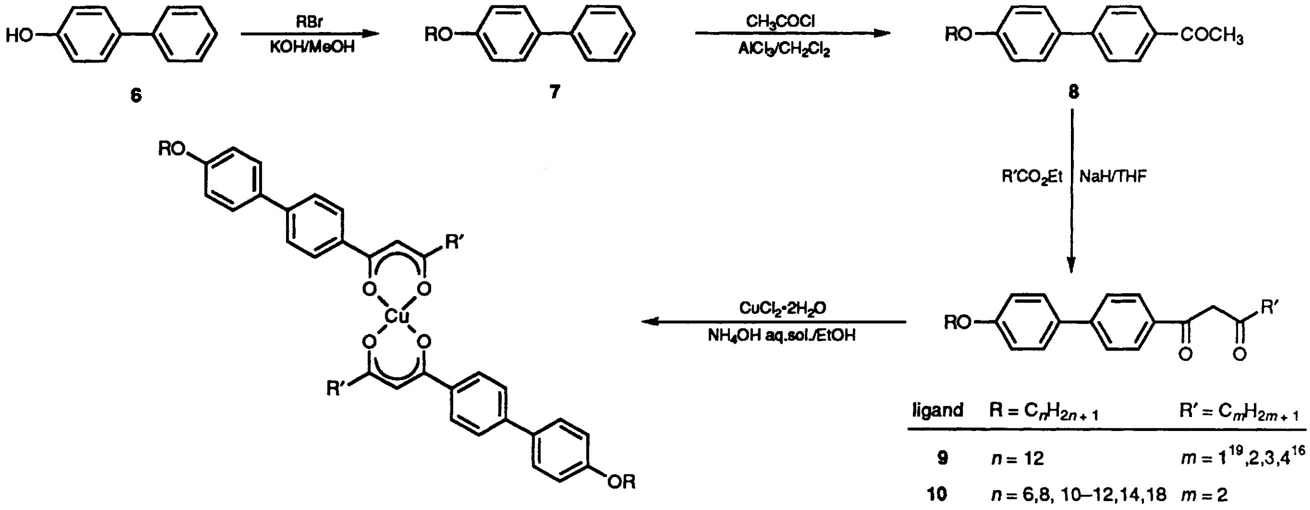

ligand	R = C_nH_{2n+1}	R′ = C_mH_{2m+1}
9	n = 12	m = 1[19],2,3,4[16]
10	n = 6,8, 10–12,14,18	m = 2

complex	R = C_nH_{2n+1}	R′ = C_mH_{2m+1}
11	n = 12	m = 1[11],2,3,4[16]
12	n = 6,8, 10–12,14	m = 2

Scheme 1 Synthetic route of 1-(4′-alkokoxybiphenyl-4-yl)-3-alkylpropane-1,3-diones (**9** and **10**) and their corresponding copper(II) complexes (**11** and **12**)

Table 1 Elemental analysis data and yields of **9** and **10**

			elemental analysis (%) found (calc.)		
	m or *n*	formula	C	H	yield (%)
9	3	$C_{30}H_{42}O_3$	79.95 (79.92)	9.39 (9.27)	38
10	6	$C_{23}H_{28}O_3$	78.38 (78.26)	8.01 (7.98)	35
	8	$C_{25}H_{32}O_3$	78.91 (79.13)	8.48 (8.46)	58
	10	$C_{27}H_{36}O_3$	79.37 (79.58)	8.88 (8.89)	56
	11	$C_{28}H_{38}O_3$	79.58 (79.66)	9.06 (9.06)	68
	12	$C_{29}H_{40}O_3$	79.77 (79.92)	9.32 (9.27)	38
	14	$C_{32}H_{44}O_3$	80.13 (80.34)	9.54 (9.65)	69
	18	$C_{35}H_{52}O_3$	80.72 (80.95)	10.06 (10.07)	89

Table 2 Elemental analysis data and yields of **11** and **12**

			elemental analysis (%) found (calc.)		
	m or *n*	formula	C	H	yield (%)
11	3	$C_{60}H_{82}O_6Cu$	74.85 (75.17)	8.58 (8.65)	64
12	6	$C_{46}H_{54}O_6Cu$	72.08 (71.81)	7.10 (7.06)	66
	8	$C_{50}H_{62}O_6Cu$	73.00 (73.30)	7.60 (7.68)	65
	10	$C_{54}H_{70}O_6Cu$	73.81 (73.44)	8.03 (7.97)	19
	11	$C_{56}H_{74}O_6Cu$	74.18 (74.01)	8.23 (8.28)	45
	12	$C_{58}H_{78}O_6Cu$	74.52 (74.28)	8.41 (8.30)	64
	14	$C_{62}H_{56}O_6Cu$	75.15 (75.34)	8.75 (8.81)	75

plate controlled by a thermoregulator (Mettler FP80 and FP82) and measured with a differential scanning calorimeter (Rigaku Thermoflex TG-DSC). The X-ray diffraction measurements on the powder were performed with Cu-Kα radiation, using a Rigaku Geigerflex equipped with a hand-made heating plate controlled by a thermoregulator. Conoscopic observations were made with a hand-made heater with a hole (the diameter is 3.0 mm), Sakaguchi-Dennetsu Samiconheater Super 350, and a temperature controller (Chino KP1250BR00). The sample was sandwiched between two commercially available cover slips (each of thickness *ca.* 0.15 mm) with a spacer (50 or 100 μm, Teijin Tetron Film). The internal surfaces were without any treatments of silane. For the case of 100 μm thickness, the cell was further sandwiched between two aluminium plates (thickness: top = *ca.* 0.3 mm; bottom = *ca.* 1.5 mm) having a hole (diameter 3.0 mm) in the centre; a d.c. voltage was applied (*ca.* 200 V) using a V-C stabilizer (Mitsumi Scientific Industry Co., Ltd, SJ-1051).

Results and Discussion

Mesomorphism of the Ligands

1-(4'-*Dodecyloxybiphenyl*-4-yl)-3-*alkylpropane*-1,3-*diones* (**9**)

In Table 3 are summarized the phase-transition temperatures and phase-transition enthalpy changes for the ligand **9** (R' = C_mH_{2m+1}, $m = 1$–4). The mesomorphism of the derivatives **9** $m = 1$ and $m = 4$ has already been described in our previous papers.[16,19] Here we synthesized **9** with $m = 2$ and with $m = 3$ and investigated their mesomorphic properties. The derivative **9** ($m = 2$) has two enantiotropic mesophases, E and S_A, similar to the **9** ($m = 1$) derivative. The **9** ($m = 3$) derivative has monotropic E and enantiotropic S_A mesophases similar to the **10** ($n = 18$) compound. The **9** ($m = 4$) derivative has only an S_A phase. Thus, for the derivatives **9** the E phase tends to disappear for $m \geqslant 3$. It can be thought that the longer the R' group of ligand **9**, the more freely the molecules rotate in the layer, because the R' groups can disturb the molecular assembly, as shown in Fig. 2.

Table 3 Phase transition temperatures (T) and enthalpy changes (ΔH) of **9** ($m = 1$–4)

m phase [a] $\xrightarrow{T/°C\ (\Delta H/\text{kcal mol}^{-1})}$ phase

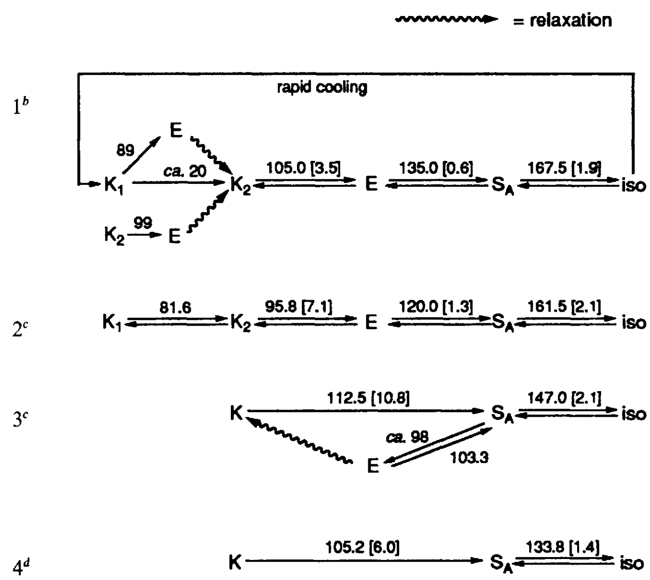

[a]Phase nomenclature: K = crystal, E = E phase, S_A = smectic A phase and iso = isotropic liquid. [b]Reference 19. [c]This work. [d]Reference 16.

1-(4'-*Alkoxybiphenyl*-4-yl)*pentane*-1,3-*dione* (**10**)

Each of these derivatives ($n = 6$, 8, 10–12, 14, 18) has both E and smectic A (S_A) phases. Their phase-transition temperatures and phase-transition enthalpy changes are summarized in Table 4. In Fig. 3 all transition temperatures for **10** are plotted against the number of carbon atoms in the alkoxy chain. The detailed mesomorphism of the representative compounds **10** ($n = 8$) and **10** ($n = 18$), are described as follows.

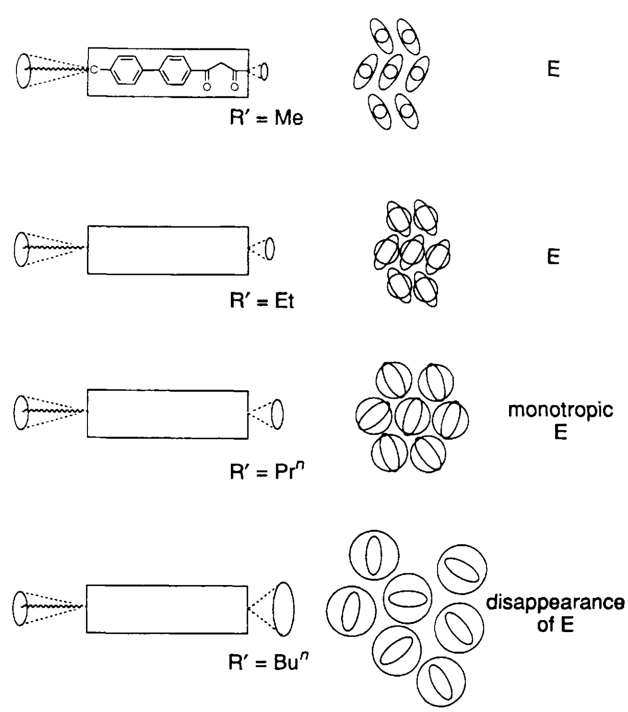

Fig. 2 Possible reason for the disappearance of the E phase in **9** when the *n*-alkyl chain becomes longer

Table 4 Phase-transition temperatures (T) and enthalpy changes (ΔH) of **10**.

n	phase [a] $\xrightarrow{T/°\mathrm{C}\ (\Delta H/\mathrm{kcal\ mol^{-1}})}$ phase

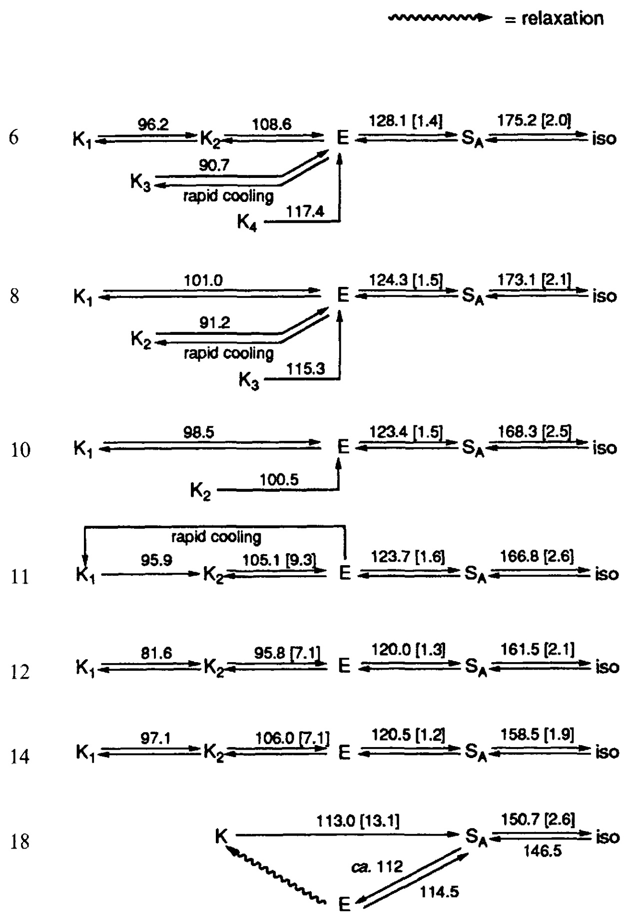

[a] Phase nomenclature: K = crystal, E = E phase, S_A = smectic A phase and iso = isotropic liquid.

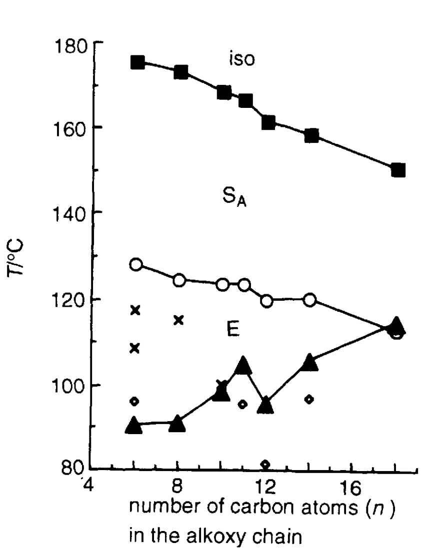

Fig. 3 Phase-transition temperature vs. number of carbon atoms in the n-alkoxy chain of **10**: ■, clearing point; ○, E–S_A transition; ▲, melting point; ◇, solid–solid transition; x, undefined phase transition

1(-4′-*Octyloxybiphenyl*-4-yl)*pentane*-1,3-*dione* [**10** (n=8)]. When the K_3 crystals of **10** (n=8) were heated from room temperature (r.t.), they melted to an E phase at 115.3 °C, followed by an S_A phase at 124.3 °C; on further heating, the S_A phase cleared into an isotropic liquid (iso) at 173.1 °C. The textures of the two mesophases are shown in Plate 1. When the isotropic liquid (iso) was cooled to 169.9 °C, a focal–conic fan texture appeared. Plate 1(*a*) was obtained on cooling to 130.0 °C; this texture consists of the parts of focal–conic fans and homeotropic arrangement characteristic of the S_A phase. When the sample of Plate 1(*a*) was cooled to 119.0 °C, the focal–conic fans changed to the arced focal–conic fans and the homeotropic arrangement part changed to a mosaic texture, as shown in Plate 1(*b*); the texture is often observed for the E phase.

These E and S_A mesophases were confirmed by X-ray powder diffraction. The patterns are shown in Fig. 4 and the data are given in Table 5. The X-ray diffraction powder

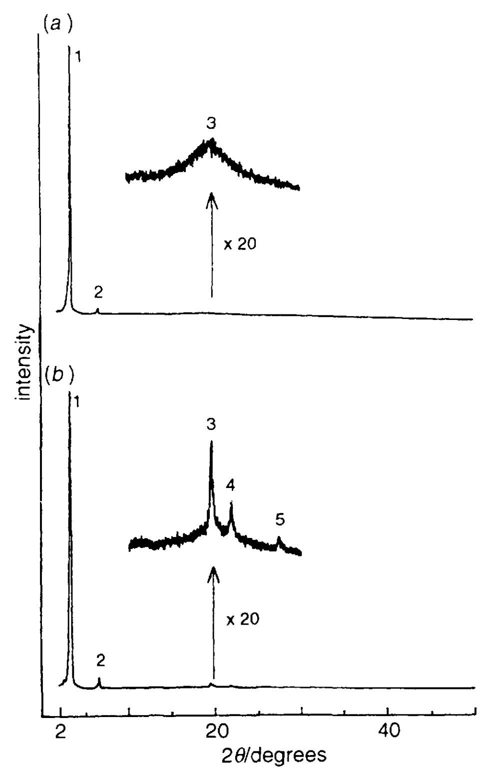

Fig. 4 X-Ray powder diffraction patterns of **10** (n=8): (*a*) the S_A phase at 155 °C, (*b*) the E phase at 122 °C

Table 5 X-Ray diffraction data of **10** (n-8): (*a*) the S_A phase at 155 °C, (*b*) the E phase at 122 °C

peak no.	$d_{obs.}$/Å	$d_{calc.}$/Å	Miller indices ($h\ k\ l$)
	(*a*) c=25.9Å		
1	24.7	25.9	(0 0 1)
2	12.9	12.9	(0 0 2)
3	*ca.* 4.5	—	melt of the alkoxy chains
	(*b*) a=8.11 Å; b=5.47 Å, c=26.2 Å		
1	25.2	26.2	(0 0 1)
2	13.1	13.1	(0 0 2)
3	4.54	4.54	(1 1 0)
4	4.06	4.06	(2 0 0)
5	3.26	3.26	(2 1 0)

pattern of the S_A phase at 155 °C [Fig. 4(*a*)] has two narrow reflections in the X-ray low-angle region, which correspond to the (001) and (002) planes for a layered structure. The interlayer distance is 25.9 Å. It also has a diffuse band around $2\theta=20°$ in the wide-angle region, corresponding to the melt of the alkoxy chains (peak no. 3). Since it has a layered structure without any order in the layer, this higher-temperature mesophase was identified as either an S_A or an S_C phase. The phase has a focal–conic fan texture. It was concluded that it was an S_A phase. In Fig. 4(*b*) the X-ray diffraction powder pattern of the E phase at 122 °C is shown. It has two narrow reflections in the low-angle region, which correspond to the (001) and (002) planes; the interlayer distance is 26.2 Å. It also has three narrow reflections on a diffuse element in the wide-angle region, which correspond to the (110), (200) and (210) planes in a two-dimensional rectangular lattice; the lattice constants are $a=8.11$ Å and $b=5.49$ Å. Thus, the lower-temperature mesophase was confirmed as an E phase.

1-(4′-*Octadecyloxybiphenyl*-4-yl)*pentane*-1,3-*dione* [**10** ($n=18$)]. This derivative shows different phase-transition behaviour from the other compounds **10**. It exhibits a monotropic E and an enantiotropic S_A mesophase. Thus, the E phase of the derivatives **10** with $n \geqslant 18$ may have a tendency to disappear (Fig. 3). From a thermodynamic viewpoint, the disappearance of the E phase results from a balance of stabilities of the E and crystal phases and is attributed to the increased stability of the crystal phase with increasing chain length. Here we wish to discuss the disappearance of the E phase from the viewpoint of molecular shape and molecular rotation.

Molecules in a layer of the E phase cannot rotate freely around the molecular axis (Fig. 5, top left). The molecules can oscillate through angles of $<180°$.[20] If the molecules can rotate freely, the mesophase may change to another mesophase such as an S_A phase which has no order in the layer (Fig. 5, top right). Goodby and Gray discussed the structure of the E phase in the *n*-alkyl 4′-*n*-alkoxybiphenyl-4-carboxylates and its relationship to molecular structure, in a very similar way to ours.[21] The present molecule of derivative **10** can be assumed to consist of two parts, that is a soft hydrocarbon chain contributing to the free rotation (*a*) and a rigid strip-like plane contributing to make the two-dimensional rectangular lattice of the E phase (*b*) (Fig. 6, bottom). With an increasing number (*n*) of carbon atoms in the alkoxy chain, the ratio $r=a/b$ increases and the molecules can rotate more easily. In this case, the tight lattice of the E phase is no longer maintained; the E phase may disappear.

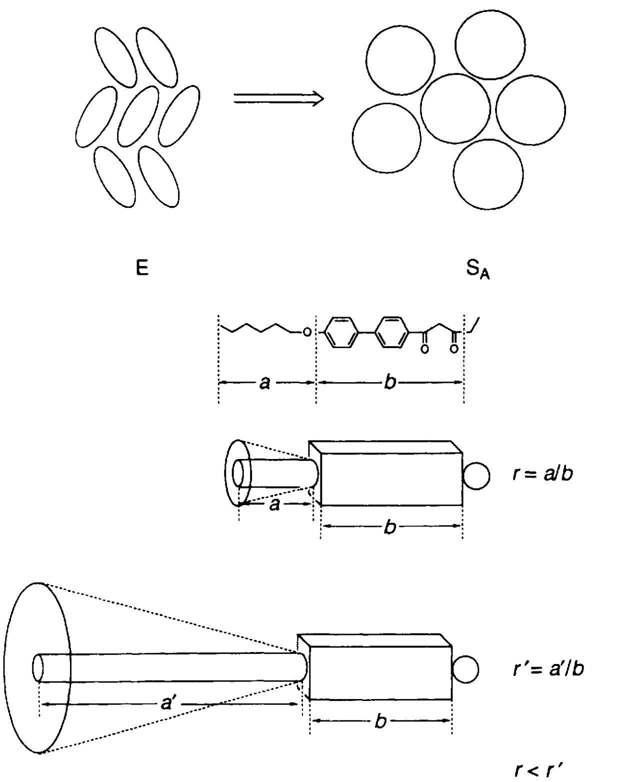

Fig. 5 Possible reason for the disappearance of the E phase in **10** when the *n*-alkoxy chain becomes longer

Mesomorphism of the Copper Complexes

Complexes 11

In Table 6 are summarized the phase-transition temperatures and phase-transition enthalpy changes for complexes **11** ($R'=C_mH_{2m+1}$, $m=1$–4). We have already reported in our previous papers[11,16] that the $m=1$ complex shows a discotic rectangular ordered columnar (D_{ro} mesophase, and that the $m=4$ complex show a monotropic N phase. The complexes with $R'=C_2H_5$ ($m=2$) and $R'=n\text{-}C_3H_9$ ($m=3$) synthesized here show an enantiotropic N phase. A temperature range of the N phase for $R'=n\text{-}C_3H_9$ is extremely narrow in comparison with that for $R'=C_2H_5$. The nematic phase of these complexes shows both a *Schlieren* texture and a marbled texture characteristic of the nematic phase (Plate 2). These complexes show double melting behaviour *via* the nematic phase.[21] For this behaviour, the accurate phase-transition enthalpy changes could not be measured (Table 6). As can be seen in Table 6, the change from the D_{ro} phase into the N phase critically occurs with changing from R′ = methyl group to R′ = ethyl group, and the N phase has a tendency to disappear when the substituent R′ is longer.

We considered the effect of the alkyl chain (R′) on meso-

Table 6 Phase-transition temperatures (*T*) and enthalpy changes (ΔH) of **11**

R′	phase[a] $\xrightarrow[\Delta H/\text{kcal mol}^{-1}]{T/°C}$ phase
	⇝ = relaxation
CH_3[b]	$K \xrightarrow{135.1} D_{ro} \xrightarrow{208.8}$ iso (decomp)
C_2H_5	$K_1 \rightarrow K_2 \rightleftharpoons^{171.9} N \rightleftharpoons^{183.6}_{0.2}$ iso; $K_1 \xrightarrow{171.3} N \rightsquigarrow K_2$
$n\text{-}C_3H_7$	$K_1 \rightarrow K_2 \rightleftharpoons^{159.9} N \rightleftharpoons^{160.0}$ iso; $K_1 \xrightarrow{159.5} N \rightsquigarrow K_2$
$n\text{-}C_4H_9$[c]	$K_1 \xrightarrow{111.5} K_2 \xrightarrow{153.3}$ iso; iso $\xrightarrow{\text{rapid cooling}}$ N; N $\rightsquigarrow K_2$ (fast); $K_2 \to$ N (very slow)

[a]Phase nomenclature: K = crystal, D_{ro} = discotic rectangular ordered columnar mesophase, N = nematic, and iso = isotropic liquid. [b]Reference 11. [c]Reference 16.

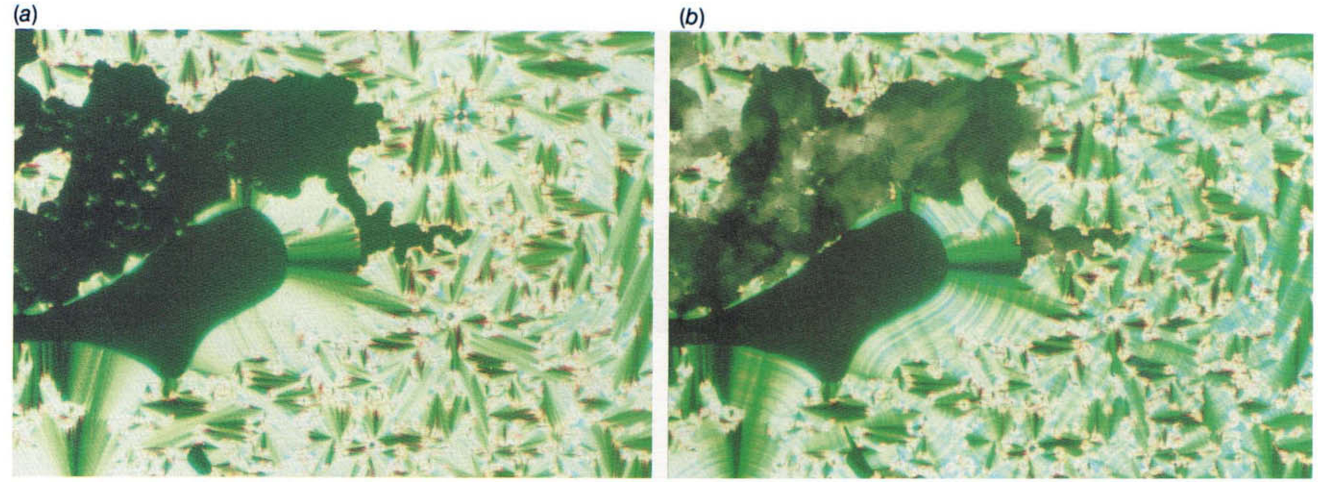

Plate 1 Textures of the mesophases of **10** ($n=8$): (*a*) the focal–conic fan texture of the S_A mesophase obtained from the isotropic liquid on cooling to 130 °C; (*b*) the arced focal–conic fan texture and mosaic texture of the E mesophase obtained from the S_A on cooling to 119 °C

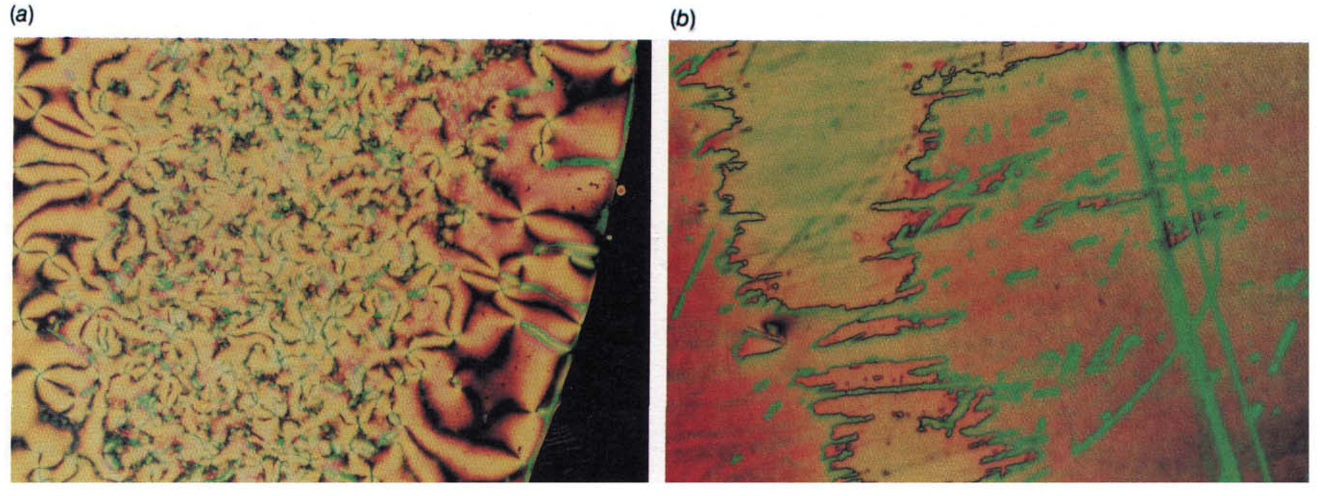

Plate 2 Textures of the nematic phase of **11** ($m=3$): (*a*) *Schlieren* texture and (*b*) marbled texture

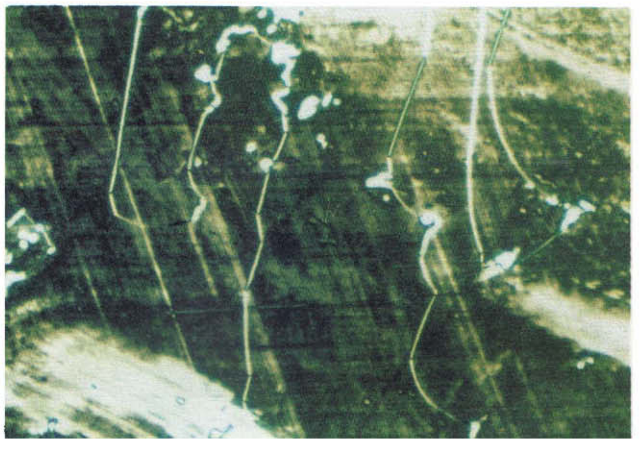

Plate 3 Zigzag disclination in the nematic phase of **12** ($n=14$)

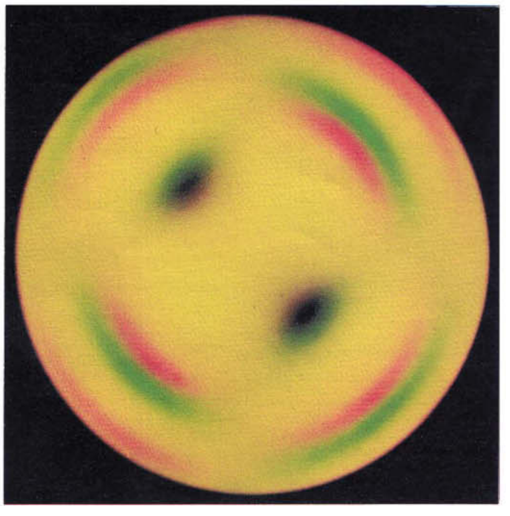

Plate 5 Conoscopic observation of the nematic phase of **12** ($n=14$) with the $1/4\lambda$ plate

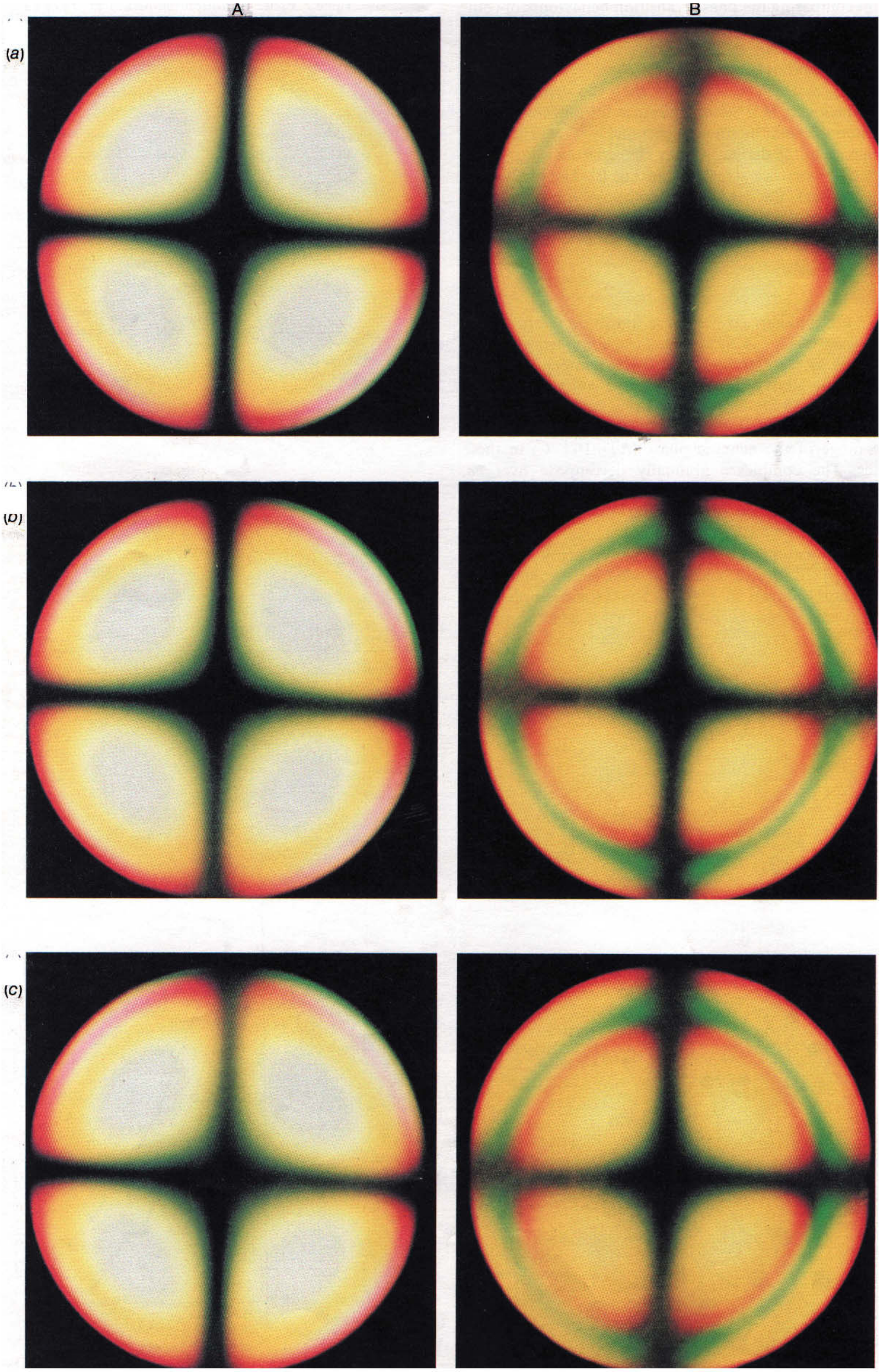

Plate 4 Conoscopic observation showing the uniaxiality of the nematic phase of **12** ($n=14$). A, Thickness $=50$ μm, spontaneous homeotropic alignment; B, thickness $=100$ μm, d.c. $=200$ V. (*a*) 0°; (*b*) 45°; (*c*) 90°

morphism comparing the phase-transition behaviours of complexes **11**. As illustrated in Fig. 6 stage 1, the molecules of **11** ($m=1$) form dimers in the D_{ro} mesophase.[11] When the R′ group in the vicinity of the core of the complex is substituted by an ethyl group, which is bulkier than the methyl group, this substituent acts as a steric hindrance for forming dimers, and the intermolecular interaction becomes weaker. Therefore, the mesophase of the derivative may change from a D_{ro} phase to a nematic phase (See stage 1→2 in Fig. 6). The bulkier the R′ group becomes, the weaker the intermolecular interaction becomes. Hence, the nematic phase may hardly appear and an isotropic liquid phase may appear before the nematic phase (stage 2→3).

Complexes **12**

In Table 7 are summarized the phase-transition temperatures for **12**($n=6$, 8, 10–12, 14). In Fig. 7, all transition temperatures of derivatives **12** were plotted against the number of carbon atoms (n) in the alkoxy chain. All of these complexes have a nematic phase, and show double-melting behaviour *via* the nematic phase.[15,22] The $n=11$ derivative has the widest temperature range of the nematic phase ($\Delta T=16.1$ °C) in these complexes. The complexes gradually decompose over *ca.* 200 °C. Therefore, the derivatives of $n \leqslant 5$ were not synthesized, although they could possibly exhibit the nematic phase above 200 °C.

The optical textures of these complexes are a *Schlieren* texture, a marbled texture, and a threaded texture, similar to the photographs shown in Plate 2. Thus, the mesophase of these complexes could be established as a nematic phase.

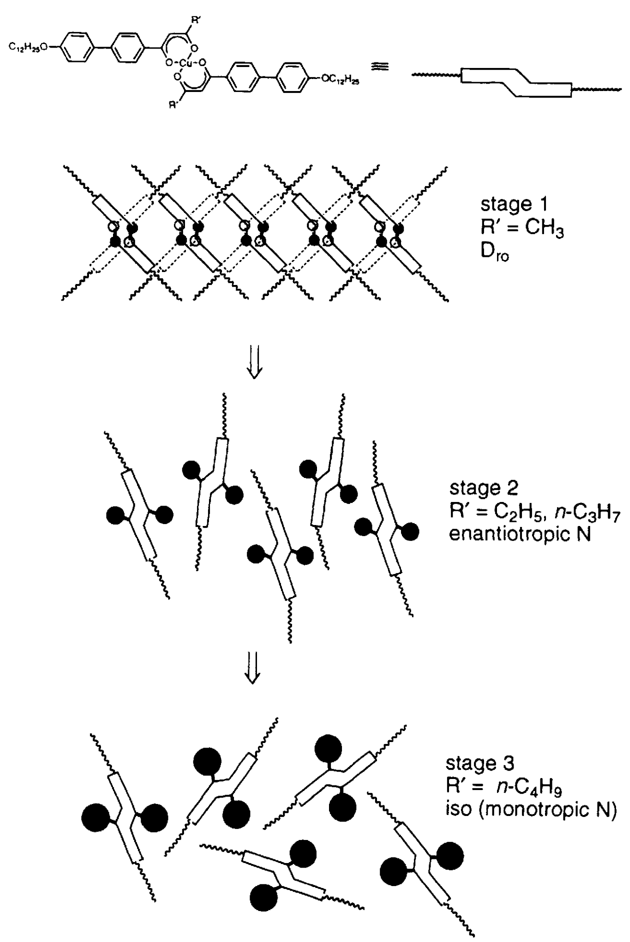

Fig. 6 Possible reason of the n-alkyl chain effect on the mesomorphism in **11**

Table 7 Phase-transition temperatures (T) of **12**

(phase[b] $\xrightarrow{T/°C}$ phase; ⇝ = relaxation)

n	$K_1 \rightarrow N$ ($N \rightsquigarrow K_2$)	$K_1 \rightarrow K_2$	$K_2 \rightarrow N$	$N \rightarrow$ iso
6	216.5		218.9	223.6 iso (decomp)
8	189.3		196.6	211.2 iso (decomp)
10	181.5		182.4 ($\rightleftharpoons$)	195.3 ($\rightleftharpoons$) iso[a]
11	172.6		173.2 ($\rightleftharpoons$)	189.3 ($\rightleftharpoons$) iso[a]
12	171.3		171.9 ($\rightleftharpoons$)	183.6 ($\rightleftharpoons$) iso[a]
14	162.5		163.5 ($\rightleftharpoons$)	175.1 ($\rightleftharpoons$) iso[a]

[a]Gradual decomposition for several heating–cooling cycles. [b]Phase nomenclature: K = crystal, N = nematic mesophase and iso = isotropic liquid.

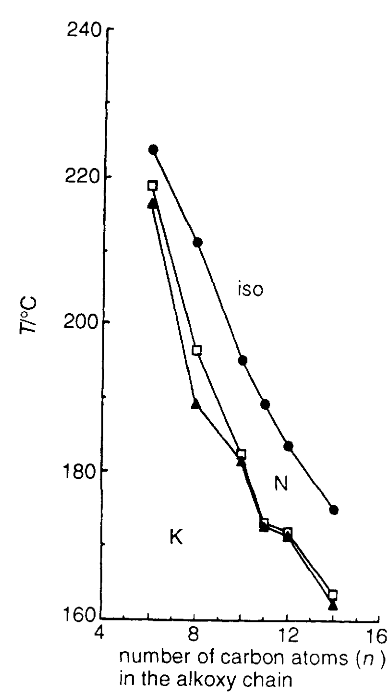

Fig. 7 Phase-transition temperatures *vs.* number of carbon atoms in the n-alkoxy chain for **12**: ●, N–iso clearing point; □, K_2–N melting point; ▲, K_1–N melting point

Interestingly, these nematic phases sometimes show a zigzag disclination texture as shown in Plate 3. When the thickness of the sample was thin, this texture could be observed.

Chandrasekhar *et al.* reported that the complex bis[1-4'-decylbiphenyl-4-yl)-3-(4-ethoxyphenyl)propane-1,3-dionato]-copper(II), whose structure is extremely similar to that of **12**, has a biaxial nematic (N_b) phase,[12–14] and exhibits also the zigzag disclination texture. Therefore, we examined the axiality of the present nematic phase by conoscopic observation. For these observations, it is necessary to align the molecules in a homeotropic structure. Surprisingly, the present nematic liquid-crystalline molecules sometimes align spontaneously in a homeotropic structure between two cover slips (a thickness $\leqslant 50$ μm) without silane coating on the surface and without applying an external electric field or a magnetic field. Therefore, it is very easy to carry out the conoscopic observations for this nematic state. Plate 4A(*a*) is a conoscopic figure for a spacer thickness of 50 μm. Though the cell was rotated by 45° [Plate 4A(*b*)] and then by 90° [Plate 4A(*c*)] on the basis of Plate 4A(*a*), the crossed lines of the conoscopic figures did not change. When the thickness of the spacer was 100 μm, the crossed lines did not change [Plate 4B(*a*)–(*c*)], as for 50 μm. In this case, the homeotropic alignment could be achieved only by applying an external electric field (d.c. 200 V). These results supported the fact that the nematic phase of the present complexes is uniaxial. Although the tilt angle of the nematic phase was not measured for these conoscopic observations, the homeotropic alignment could be supported because the crossed lines showed no change for rotating the sample.

Plate 5 is the conoscopic figure obtained when a $1/4\lambda$ plate was inserted for the sample of Plate 4B(*a*). It can be concluded from this figure that the present nematic phase is optically positive.

Conclusions

We have investigated the mesomorphic properties of compounds **9** and **10**. It was found that each of the derivatives **10** for $n=6$–14 has both enantiotropic E and S_A phases but the derivative for $n=18$ gives a monotropic E phase and an enantiotropic S_A phase. On the other hand, the derivatives **9** for $m=1$ and 2 have both the enantiotropic E phase and the S_A phase, whereas they have a monotropic E phase and an enantiotropic S_A phase for $m=3$ and only an enantiotropic S_A phase for $m=4$. Therefore, it is apparent that the E phases of both **9** and **10** have a tendency to disappear when the alkoxy/alkyl group is elongated.

As reported in the previous papers, complex **11** has a D_{ro} phase[11] for R' = methyl group and the complex has a monotropic N phase for R' = *n*-butyl group.[16] The complexes with an R' = ethyl group or an R' = *n*-propyl group synthesized in this work show an enantiotropic N phase. Therefore, the change from the D_{ro} phase to the N phase in complexes **11** critically occurs with changing from R' = methyl group to R' = ethyl group. The N phase has a tendency to disappear when the substituent R' is longer.

All of the derivatives **12** have an enantiotropic nematic phase, and show double-melting behaviour *via* the nematic phase. The $n=11$ derivative has the widest temperature range of the nematic phase in these complexes. The nematic phase of these complexes was established as an optically positive uniaxial nematic phase, although it showed a zigzag disclination texture.

References

1 K. Ohta, Y. Morizumi, T. Fujimoto, I. Yamamoto, K. Miyamura and Y. Gohshi, *Mol. Cryst. Liq. Cryst.*, 1992, **214**, 161.
2 A. M. Giroud-Godquin and J. Billard, *Mol. Cryst. Liq. Cryst.*, 1981, **61**, 147.
3 A. M. Giroud-Godquin and J. Billard, *Mol. Cryst. Liq. Cryst.*, 1983, **97**, 287.
4 J. Billard, *C. R. Acad. Sci. Paris*, 1984, **299**, 905.
5 K. Ohta, A. Ishii, I. Yamamoto and K. Matsuzaki, *J. Chem. Soc., Chem. Commun.*, 1984, 1099; K. Ohta, A. Ishii, I. Yamamoto and K. Matsuzaki, *Mol. Cryst. Liq. Cryst.*, 1985, **116**, 299.
6 K. Ohta, H. Muroki, A. Takagi, I. Yamamoto and K. Matsuzaki, *Mol. Cryst. Liq. Cryst.*, 1986, **135**, 247.
7 B. K. Sadashiva and S. Ramesha, *Mol. Cryst. Liq. Cryst.*, 1986, **141**, 19.
8 K. Ohta, H. Muroki, A. Takagi, K. Hatada, H. Ema, I. Yamamoto and K. Matsuszaki, *Mol. Cryst. Liq. Cryst.*, 1986, **140**, 131; K. Usha, K. Vijayan and B. K. Sadashiva, *Mol. Cryst. Liq. Cryst. Lett.*, 1987, **5**, 67; H. Sakashita, A. Nishitani, Y. Sumiya, K. Ohta and I. Yamamoto, *Mol. Cryst. Liq. Cryst.*, 1988, **163**, 211.
9 A. M. Giroud-Godquin, G. Sigaud, M. F. Achard and H. Hardouin, *J. Phys. Lett.*, 1984, L-387; A. M. Giroud-Godquin, M. M. Gauthier, G. Sigaud, F. Hardouin and M. F. Achard, *Mol. Cryst. Liq. Cryst.*, 1986, **132**, 35.
10 K. Ohta, H. Ema, H. Muroki, I. Yamamoto and K. Matsuzaki, *Mol. Cryst. Liq. Cryst.*, 1987, **147**, 61.
11 K. Ohta, O. Takenaka, H. Hasebe, Y. Morizumi, T. Fujimoto and I. Yamamoto, *Mol. Cryst. Liq. Cryst.*, 1991, **195**, 135.
12 S. Chandrasekhar, B. K. Sadashiva and B. S. Srikanta, *Mol. Cryst. Liq. Cryst.*, 1987, **151**, 93.
13 S. Chandrasekhar, B. R. Ranta, B. K. Sadashiva and V. N. Raja, *Mol. Cryst. Liq. Cryst.*, 1988, **165**, 123.
14 S. Chandrasekhar, V. N. Raja and B. K. Sadashiva, *Mol. Cryst. Liq. Cryst., Lett.*, 1990, **7**, 65.
15 B. Mühlberger and W. Haase, *Liq. Cryst.*, 1989, **5**, 251.
16 K. Ohta, O. Takenaka, H. Hasebe, Y. Morizumi, T. Fujimoto and I. Yamamoto, *Mol. Cryst. Liq. Cryst.*, 1991, **195**, 123.
17 N. J. Tompson, G. W. Gray, J. W. Goodby and K. J. Toyne, *Mol. Cryst. Liq. Cryst.*, 1991, **200**, 109.
18 G. W. Gray, B. Jones and F. Marchon, *J. Chem. Soc.*, 1957, 393.
19 K. Ohta, O. Takenaka, H. Hasebe, Y. Morizumi, T. Fujimoto and I. Yamamoto, *Mol. Cryst. Liq. Cryst.*, 1991, **195**, 103.
20 G. W. Gray and J. W. Goodby, *Smectic Liquid Crystals, Textures and Structures*, Leonard Hill, Glasgow, 1984, ch. 5, pp. 83–88.
21 J. W. Goodby, *Mol. Cryst. Liq. Cryst.*, 1981, **75**, 179; J. W. Goodby and G. W. Gray, *Mol. Cryst. Liq. Cryst.*, 1978, **48**, 127; G. W. Gray and J. W. Goodby, *Mol. Cryst. Liq. Cryst.*, 1976, **37**, 157.
22 C. L. Hilleman, G. R. Van Hecke, S. R. Peak, J. B. Winther, M. A. Rudat, D. A. Kalman and M. L. White, *J. Phys. Chem.*, 1975, **79**, 1566; C. L. Hilemann and G. R. Van Hecke, *J. Phys. Chem.*, 1976, **80**, 944; K. Ohta, H. Ema, Y. Morizumi, T. Watanabe, T. Fujimoto and I. Yamamoto, *Liq. Cryst.*, 1990, **8**, 311.

Paper 3/01024D; *Received* 19*th February*, 1993